AIP | Applied Physics Letters

Photonic crystal membrane reflectors by magnetic field-guided metal-assisted chemical etching

Karthik Balasundaram, Parsian K. Mohseni, Yi-Chen Shuai, Deyin Zhao, Weidong Zhou, and Xiuling Li

Citation: Applied Physics Letters **103**, 214103 (2013); doi: 10.1063/1.4831657
View online: http://dx.doi.org/10.1063/1.4831657
View Table of Contents: http://scitation.aip.org/content/aip/journal/apl/103/21?ver=pdfcov
Published by the AIP Publishing

Photonic crystal membrane reflectors by magnetic field-guided metal-assisted chemical etching

Karthik Balasundaram,[1] Parsian K. Mohseni,[1] Yi-Chen Shuai,[2] Deyin Zhao,[2] Weidong Zhou,[2,a)] and Xiuling Li[1,a)]
[1]*Micro and Nanotechnology Laboratory, Department of Electrical and Computer Engineering, University of Illinois at Urbana-Champaign, Urbana, Illinois 61801, USA*
[2]*Department of Electrical Engineering, NanoFAB Center, University of Texas at Arlington, Arlington, Texas 76019, USA*

(Received 26 September 2013; accepted 31 October 2013; published online 20 November 2013)

Metal-assisted chemical etching (MacEtch) is a simple etching method that uses metal as the catalyst for anisotropic etching of semiconductors. However, producing nano-structures using MacEtch from discrete metal patterns, in contrast to interconnected ones, has been challenging because of the difficulties in keeping the discrete metal features in close contact with the semiconductor. We report the use of magnetic field-guided MacEtch (*h*-MacEtch) to fabricate periodic nanohole arrays in silicon-on-insulator (SOI) wafers for high reflectance photonic crystal membrane reflectors. This study demonstrates that *h*-MacEtch can be used in place of conventional dry etching to produce ordered nanohole arrays for photonic devices. © *2013 AIP Publishing LLC*. [http://dx.doi.org/10.1063/1.4831657]

Metal-assisted chemical etching (MacEtch) is a wet but directional etching technique which involves a thin layer of noble metal (e.g., Au, Pt, etc.) acting as a catalyst to guide the etch process in a solution that usually consists of an oxidant and an acid. The role of the catalyst metal is to selectively enhance the rate of oxidation of the semiconductor underneath, whereas the region outside the metal patterns has a larger energy barrier for this oxidation reaction to take place. The role of the acid is to dissolve the oxidized semiconductor species to allow continued oxidation and etching in the direction normal to the metal-semiconductor interface. Details of the MacEtch mechanism can be found elsewhere.[1–3] In recent years, several research groups have demonstrated the use of MacEtch for the fabrication of micro/nanostructures of various aspect ratios and surface morphologies using both Si and compound semiconductors.[1,4–9] As the technique relies on patterning of a thin noble metallic catalyst layer, which sinks down and engraves into the semiconductor during etching, the semiconductor structures formed using MacEtch are exactly complementary to the metal patterns. Therefore, metal mesh patterns produce vertical pillars[4,8–10] and discrete metal particles yield cylindrical holes.[11] While vertical nanopillar arrays fabricated using MacEtch have been shown for energy harvesting[3,12] and light emitting diode (LED)[9] applications, devices relying on MacEtched nanohole arrays have been more elusive. The fabrication of periodic arrays of nanoholes using MacEtch can extend the use of this simple and low-cost technique to the field of optics and nanophotonics for the formation of nanoscale patterned structures and cavities, such as photonic crystals (PhCs) and functional semiconductor metamaterials, currently being made largely by plasma-assisted dry etching processes.[13,14]

A few groups have reported the MacEtch of randomly distributed holes in bulk Si using metal nanoparticles formed by electroless deposition,[15–17] which limits the use of this approach only to applications where a periodic arrangement of holes is not required. However, for the formation of PhCs and metamaterials, uniform etching of an array of holes of sub-micron scale dimensions with precisely defined lattice configurations is critical. Unlike the formation of vertical pillars using a metal mesh layer as the catalyst, drilling an array of holes with uniform depth using isolated catalyst patterns is more challenging due to the lack of connectivity and, thus, coherence between the neighboring metal disks while descending. This necessitates the modification of conventional MacEtch methods reported to date to be used for the drilling of holes in Si and other semiconductor materials with controlled lattice configurations.

In 2012, Oh *et al.* reported direction-guided, nano/micro shaping of Si using an applied magnetic field for intentionally changing the direction of motion of the catalyst during MacEtch, resulting in the formation of sheets, needles, and zigzag wires.[18] This work motivated us to explore magnetic field-guided MacEtch (*h*-MacEtch) to overcome the challenges in using isolated metal catalysts for the formation of periodic arrays of holes. Such a field-guided MacEtch process can lead to the formation of straight air hole arrays with high aspect ratios, as well as, curved air holes with controlled chirality. In this letter, we report a systematic study of the etch parameters required for the fabrication of periodic nanohole arrays of sub-micron dimensions on silicon-on-insulator (SOI) wafers using MacEtch under the influence of an external magnetic field. We then demonstrate the fabrication of high performance two-dimensional (2D) air hole array PhC Si membrane reflectors (Si-MRs) using this approach.

As shown schematically in Fig. 1(a), a square-lattice air hole PhC structure on an SOI substrate was used for the Si-MRs. The key lattice parameters are shown in Fig. 1(b), where *r*, *a*, and *t* represent air hole radius, lattice constant (period), and Si-MR thickness, respectively. The design was based on rigorous coupled-wave analysis (RCWA) techniques.[13,14] For

a)Authors to whom correspondence should be addressed. Electronic addresses: wzhou@uta.edu and xiuling@illinois.edu

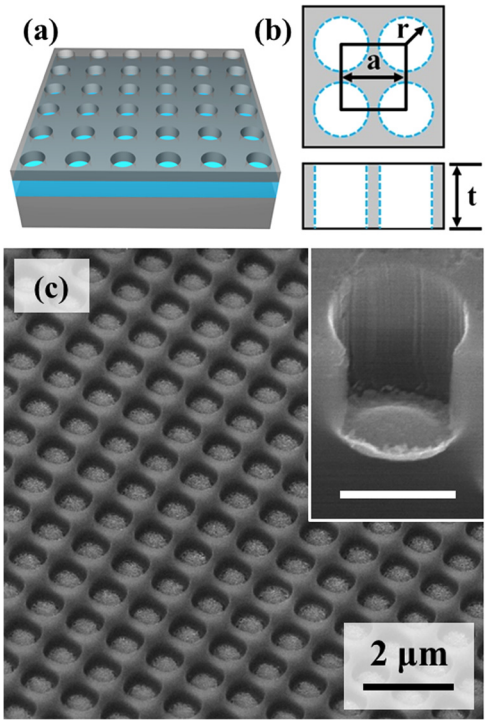

FIG. 1. (a) 3D sketch of a Si-MR with a patterned 2D air hole square-lattice PhC structure on an SOI substrate. (b) Key lattice parameters for the square-lattice air hole PhC structures are air hole radius (r), lattice constant or period (a), and Si-MR thickness (t). (c) 45° tilted-view SEM image of a nanohole array after a 60 s magnet-guided MacEtch process showing trilayer metal stacks displaced to the bottom of the etched Si air holes. Inset shows a tilted-view image of a single drilled nanohole with the catalyst disk at the bottom after MacEtch. Inset scale bar represents 500 nm.

the PhC Si-MR design considered here, with target reflection spectral band around 1500 nm, the design parameters are $a = 980$ nm, $r/a = 0.28$, and $t = 340$ nm.

After defining the patterns using electron-beam lithography (EBL), we deposited a trilayer stack of metals (Au (20 nm)/Ni (10 nm)/Au (5 nm)) on an SOI wafer (2 μm buried oxide (BOX) and 340 nm top Si) using electron-beam evaporation followed by liftoff to form metal disk patterns. The typical sample size was $\sim$0.5 mm $\times$ 0.5 mm. We then introduced the SOI wafer with metal disk patterns into a Teflon beaker with 49% hydrofluoric acid (HF, 5 ml), 30% hydrogen peroxide (H_2O_2, 1.25 ml), and deionized water (DI, 8 ml) for different etch periods (specified below). A stack of circular neodymium magnetic disks (Applied Magnets), with maximum measured magnetic field strength of 0.2 T, were placed underneath the beaker containing the MacEtch solution to ensure uniform and vertical drilling of holes in the active device area, by avoiding the detouring of metal catalyst disks during etching. The distance between the top surface of the magnet and the SOI wafer was $\sim$5 mm. Following MacEtch, the SOI wafers were submerged into a commercial gold etchant (Transene Co.) to completely remove the metal stack. Imaging and general inspection of post-MacEtch samples were carried out using a Hitachi S-4800 scanning electron microscope (SEM). For optical reflectivity measurements, a white light source (covering 1100–1700 nm spectral range) and an optical spectrum analyzer were used to measure the reflection spectra over a wide spectral bandwidth.

Fig. 1(c) shows a tilted-view SEM image of a nanohole array (diameter = 550 nm and pitch = 1 μm) fabricated on a p-type ($\rho = 5$–$10\,\Omega \cdot$ cm) Si wafer using a 60 s MacEtch process under the influence of an externally applied magnetic field. During the course of etching, the trilayer metal disks sink vertically into the substrate (as shown in the inset) due to the influence of the applied magnetic field attracting the central Ni layer of the trilayer metal stack in a downward direction. By varying the duration of etching, this approach allows for the drilling of vertical holes of any aspect ratio, so long as an intimate contact between the catalyst disk and the underlying semiconductor substrate is preserved. In addition, by switching the polarity and duration of the applied external magnetic field, this technique can, in principle, be extended to drilling helical or spiral-shaped pits for 3D photonic device applications,[19] which cannot be achieved by other anisotropic etching processes. It should be noted that the edge roughness of the metal disk controls the smoothness of the nanohole sidewalls, due to the inherent nature of the MacEtch process.[9]

For the fabrication of PhCs in Si, the technique used must produce uniform and vertical etching of holes of any given lateral and vertical dimensions. Therefore, we designed a set of experiments varying the magnetic field strength, duration of etching, and lateral dimensions of holes, in order to determine their influence on the MacEtch process.

As Oh *et al.* reported that the applied magnetic field controls the direction of motion of the catalysts,[18] we compared the morphology of holes made using MacEtch with and without an external magnetic field. In Fig. 2(a), the nanohole array fabricated using MacEtch without an applied magnetic field clearly shows the non-vertical sinking of catalyst disks into Si, whereas the nanoholes etched with an applied magnetic field of 0.2 T, as shown in Fig. 2(b), demonstrates a near-perfect elimination of non-vertical displacement of the metal disks. We also observed that with field strengths less than 0.2 T (not shown here), there were still signs of lateral detouring. This can likely be attributed to the lack of a sufficiently localized field strength near the etch front, thereby causing the displacement of the disks. Also, we note a clear enhancement of the vertical etch rate with the introduction of a 0.2 T magnetic field, as seen in Fig. 2(b). This is a direct consequence of the additional attractive magnetic force induced upon the Ni segment of the metallic trilayer stack. Very recently, Lai *et al.* reported the mechanics of catalyst motion during MacEtch of Si by studying the van der Waals (vdW) force between the catalyst and Si during etching and its dependence on the chemistry of the solution.[20] The detouring observed in our MacEtch experiments without the applied magnetic field (Fig. 2(a)) can be attributed to the non-uniform and anisotropic nature of this vdW force, even with our optimized etching conditions having a high [HF]:[H_2O_2] ratio. The enhancement of etch rate with the application of an external magnetic field (Fig. 2(b)) can be attributed to the manipulation of both the magnitude and direction of the same attractive vdW force, which is very similar to the observations of enhanced etch rates, reported by Lai *et al.*,[20] with increasing molar concentrations of HF and H_2O_2. Therefore, with the application of a sufficiently high external magnetic field (in this case, 0.2 T) and varied etch durations, our MacEtch approach can produce vertical holes of variable aspect ratios in Si.

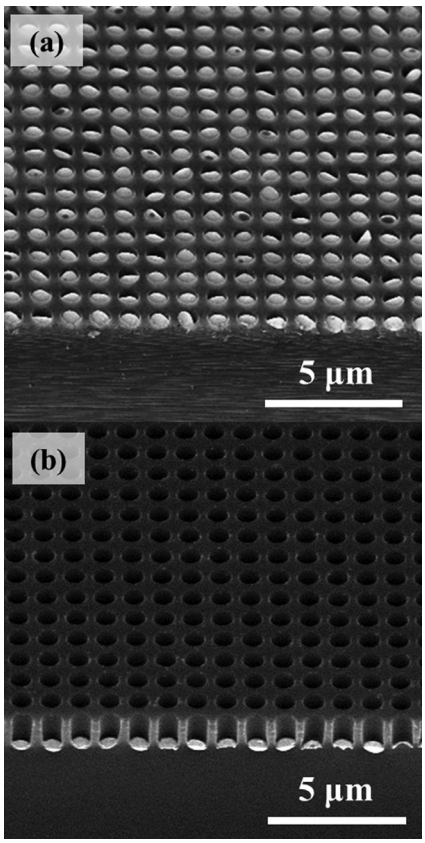

FIG. 2. 45° tilted-view SEM images of nanohole arrays after MacEtch for 60 s with (a) zero and (b) 0.2 T external magnetic field guidance.

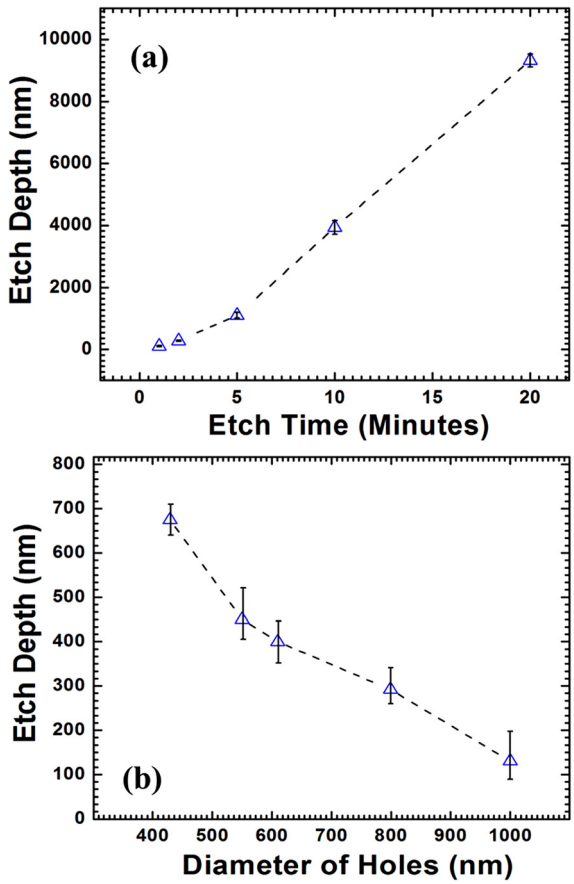

FIG. 3. Plots showing variation of etch depth with (a) duration of MacEtch for holes with diameter of 550 nm, and (b) diameter of holes under identical etch conditions for a duration of 60 s. Each data point represents the mean value measured from a sample set of 25 individual nanoholes, while error bars indicate ± one standard deviation from the mean.

The second influential parameter of interest is the duration of MacEtch. Fig. 3(a) shows the variation of etch depth as a function of etch time for nanohole arrays of 550 nm diameter and 1 μm period, made using p-type Si wafers under a constant magnetic field (0.2 T). A nearly linear trend is observed from Fig. 3(a), indicating that the vertical etch rate of such discrete features is constant. It is worth noting that a slightly lower etch rate is observed for shorter etch periods, likely the result of a latency period required for oxidation of Si at the surface. These results demonstrate that tuning of the aspect ratio of such vertical nanoholes, simply by varying the etch time, can be achieved with the proper choice of magnetic field strength.

Lastly, we consider the effect of variation of the nanohole lateral dimensions on the etch depth, for a fixed MacEtch duration and constant magnetic field. The diameter of the holes used for our study ranged from 400 to 1000 nm, as this range corresponds to the sub-wavelength regime used for the design of PhC-based devices. All samples were etched under a constant external magnetic field of 0.2 T for a fixed duration of 60 s. As shown in Fig. 3(b), the etch depth of nanoholes decreases as the diameter of the holes increases using a constant pitch of 1 μm for all samples. This decrease in etch rate can be attributed to the difference in the volume of Si atoms undergoing oxidation and removal during the MacEtch process with different lateral dimensions of the metal patterns. For etching holes in the sub-400 nm regime (not shown here), much higher etch rates can be expected as the volume of Si atoms would be reduced even further. Therefore, the current MacEtch approach may be easily scaled down to implement such design requirements.

For the SOI wafer used for our optical reflectivity measurements, we set the etch duration as 75 s in order to ensure full penetration of the catalyst disks through the top Si layer (t = 340 nm). In Fig. 4(a), a top view SEM image of a Si-MR formed on top of the BOX layer is shown. We observed that when the metal catalyst reaches the underlying BOX layer, MacEtch no longer continues, as etching of this segment proceeds isotropically in HF (no Si layers are present in the BOX to be oxidized). The patterned MRs formed using MacEtch can be released from the SOI substrate by selectively etching the BOX layer in HF, as shown in Fig. 4(b), and can be directly transferred to any other substrates based on the transfer printing technique.[21] Note that the MRs shown in the tilted-view SEM image in Fig. 4(b) had a square air hole with an alternative lattice configuration (~1 μm hole size with 2 μm period).

Fig. 5 shows the measured (solid, red curve) and simulated (dashed, blue curve) optical reflectivity spectra from a MR with a MacEtch-patterned 2D air hole square-lattice PhC structure. The parameters used for simulation to fit the experimental results are $a = 980$ nm, $r/a = 0.313$, and $t = 340$ nm. Notice that the fitted r/a value is slightly larger than the original design parameter, due to enlarged air hole sizes in the actual etched structures. Clearly, the key features in the broad high-reflection band region between the

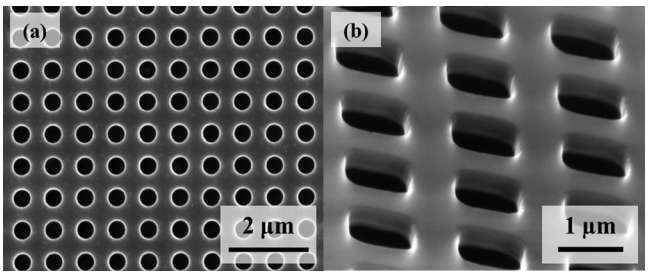

FIG. 4. (a) Top-view SEM image of a Si-MR made from an SOI wafer using magnetic field-guided MacEtch for 75 s and (b) tilted-view SEM image of a Si-MR released from the SOI wafer with an alternative lattice configuration ($\sim 1\ \mu$m hole size with $2\ \mu$m period).

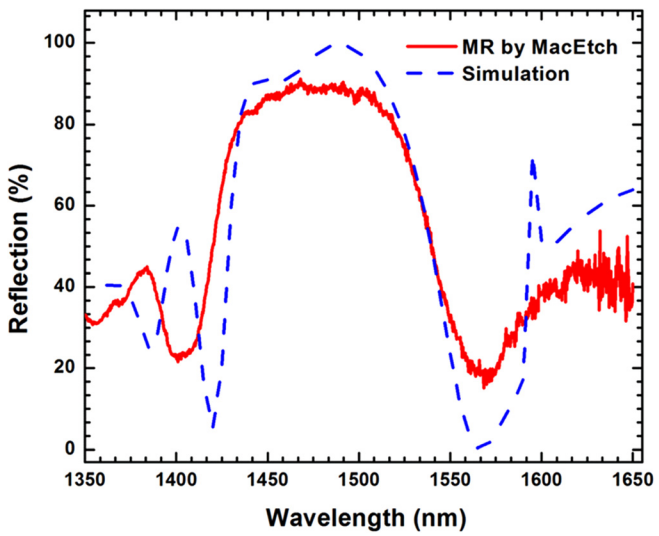

FIG. 5. Comparison of optical reflectivity data obtained by RCWA simulations (dashed, blue curve) and experimental measurements (solid, red curve) of the Si-MR fabricated by magnetic field-guided MacEtch.

experimental and simulated optical reflectivity results match very well. The measured peak value of reflectivity is approximately 90% of the simulated value at the desired wavelength of 1500 nm. Note that the Si-MR fabricated using the *h*-MacEtch approach reported here has a slightly reduced peak reflectivity compared to the Si-MRs made using dry etch approach reported earlier[22] with similar design parameters. This could be attributed to the *h*-MacEtch conditions used here, which is limited by the metal edge roughness resulting from the patterning approach and the uniformity of the magnetic field. Further improvement of the reflectivity can be achieved by minimizing the sidewall roughness and size dispersion of the etched nanoholes. Under fully optimized conditions, it is possible that the reflectivity of the device can surpass that produced by dry etch, because of the inherent damage-free nature of MacEtch. The results demonstrated here confirmed experimentally that MacEtch, a simple, low-cost, and damage-free technique, can be used for the fabrication of Si-MRs without the need for high vacuum conditions or a high thermal budget, as required for conventional plasma-assisted etching. Most importantly, the work reported here demonstrates the feasibility of the *h*-MacEtch process for fabricating high quality photonic structures, where more complicated 3D structures may be realized in the future.

In summary, we have reported the fabrication of discrete nanohole arrays in Si using magnetic field-guided MacEtch (*h*-MacEtch). We have performed a systematic study of the factors affecting the structural morphology of the holes made using this approach, including the strength of the external magnetic field, etch period, and lateral dimensions of the nanohole features. Furthermore, we have fabricated and characterized the optical reflectivity of Si-MRs using this technique. Our results show that the optical device performance of the Si-MRs made using this simple and low-cost method matches very well with theoretical models, based on RCWA simulations. Our future efforts will focus on the demonstration of spectral tunability using various dimensions of nanohole arrays. Also, we aim to apply *h*-MacEtch to the fabrication of discrete, non-linear 3D features in Si as well as compound semiconductors.

This work was supported in part by the ONR Young Investigator Program Award No. #N000141110634 (X. Li), US ARO #W911NF-09-1-0505 (W. Zhou), and by AFOSR #FA9550-08-1-0337 (W. Zhou). The authors would like to gratefully acknowledge Mr. Paul Froeter for assistance with magnetic flux density measurements.

[1]Z. Huang, N. Geyer, P. Werner, J. de Boor, and U. Gösele, Adv. Mater. **23**, 285–308 (2011).
[2]X. Li and P. W. Bohn, Appl. Phys. Lett. **77**, 2572–2574 (2000).
[3]X. Li, Curr. Opin. Solid State Mater. Sci. **16**, 71–81 (2012).
[4]W. Chern, K. Hsu, I. S. Chun, B. P. De Azeredo, N. Ahmed, K.-H. Kim, J. Zuo, N. Fang, P. Ferreira, and X. Li, Nano Lett. **10**, 1582–1588 (2010).
[5]M. DeJarld, J. C. Shin, W. Chern, D. Chanda, K. Balasundaram, J. A. Rogers, and X. Li, Nano Lett. **11**, 5259–5263 (2011).
[6]X. Geng, B. K. Duan, D. A. Grismer, L. Zhao, and P. W. Bohn, Electrochem. Commun. **19**, 39–42 (2012).
[7]Y. Yasukawa, H. Asoh, and S. Ono, Jpn. J. Appl. Phys. **49**, 116502 (2010).
[8]K. Balasundaram, J. S. Sadhu, J. C. Shin, B. Azeredo, D. Chanda, M. Malik, K. Hsu, J. A. Rogers, P. Ferreira, S. Sinha, and X. Li, Nanotechnology **23**, 305304 (2012).
[9]P. K. Mohseni, S. Hyun Kim, X. Zhao, K. Balasundaram, J. Dong Kim, L. Pan, J. A. Rogers, J. J. Coleman, and X. Li, J. Appl. Phys. **114**, 064909 (2013).
[10]J. C. Shin, C. Zhang, and X. Li, Nanotechnology **23**, 305305 (2012).
[11]K. Tsujino and M. Matsumura, Adv. Mater. **17**, 1045–1047 (2005).
[12]A. I. Hochbaum, R. Chen, R. D. Delgado, W. Liang, E. C. Garnett, M. Najarian, A. Majumdar, and P. Yang, Nature **451**, 163–167 (2008).
[13]H. Yang, D. Zhao, S. Chuwongin, J. Seo, W. Yang, Y. Shuai, J. Berggren, M. Hammar, Z. Ma, and W. Zhou, Nat. Photonics **6**, 615–620 (2012).
[14]Y. Shuai, D. Zhao, G. Medhi, R. Peale, Z. Ma, W. Buchwald, R. Soref, and W. Zhou, IEEE Photonics J. **5**, 4700206 (2013).
[15]B. Zhu, L. J. Li, Q. Q. Sun, H. L. Lu, S. J. Ding, and W. Zhang, Adv. Mater. Res. **535–537**, 362–367 (2012).
[16]K. Tsujino and M. Matsumura, Electrochem. Solid-State Lett. **8**, C193 (2005).
[17]X.-M. Zhang and N. Fukata, Solid State Commun. **156**, 76–79 (2013).
[18]Y. Oh, C. Choi, D. Hong, S. D. Kong, and S. Jin, Nano Lett. **12**, 2045–2050 (2012).
[19]C. M. Soukoulis and M. Wegener, Science **330**, 1633–1634 (2010).
[20]C. Q. Lai, H. Cheng, W. K. Choi, and C. V. Thompson, J. Phys. Chem. C **117**, 20802–20809 (2013).
[21]M. A. Meitl, Z.-T. Zhu, V. Kumar, K. J. Lee, X. Feng, Y. Y. Huang, I. Adesida, R. G. Nuzzo, and J. A. Rogers, Nature Mater. **5**, 33–38 (2005).
[22]H. Yang, D. Zhao, J. Seo, S. Chuwongin, S. Kim, J. A. Rogers, Z. Ma, and W. Zhou, IEEE Photonics Technol. Lett. **24**, 476–478 (2012).